Appl Biochem Biotechnol (2011) 164:1376–1389
DOI 10.1007/s12010-011-9219-x

glpX Gene of *Mycobacterium tuberculosis*: Heterologous Expression, Purification, and Enzymatic Characterization of the Encoded Fructose 1,6-bisphosphatase II

Hiten J. Gutka · Kamolchanok Rukseree · Paul R. Wheeler · Scott G. Franzblau · Farahnaz Movahedzadeh

Received: 29 October 2010 / Accepted: 1 March 2011 /
Published online: 31 March 2011

Abstract The *glpX* gene (*Rv1099c*) of *Mycobacterium tuberculosis (Mtb)* encodes Fructose 1,6-bisphosphatase II (FBPase II; EC 3.1.3.11); a key gluconeogenic enzyme. *Mtb* possesses *glpX* homologue as the major known FBPase. This study explored the expression, purification and enzymatic characterization of functionally active FBPase II from *Mtb*. The *glpX* gene was cloned, expressed and purified using a two step purification strategy including affinity and size exclusion chromatography. The specific activity of *Mtb* FBPase II is 1.3 U/mg. The enzyme is oligomeric, followed Michaelis–Menten kinetics with an apparent km=44 μM. Enzyme activity is dependent on bivalent metal ions and is inhibited by lithium and inorganic phosphate. The pH optimum and thermostability of the enzyme have been determined. The robust expression, purification and assay protocols ensure sufficient production of this protein for structural biology and screening of inhibitors against this enzyme.

Keywords *glpX* · Fructose 1,6–bisphosphatase · *Mycobacterium tuberculosis* · Gluconeogenesis

H. J. Gutka · K. Rukseree · S. G. Franzblau · F. Movahedzadeh (✉)
Institute for Tuberculosis Research (M/C 964), College of Pharmacy, Room 412,
University of Illinois at Chicago, 833 S. Wood St, Chicago, IL 60612–7231, USA
e-mail: movahed@uic.edu

H. J. Gutka · S. G. Franzblau · F. Movahedzadeh
Department of Medicinal Chemistry and Pharmacognosy, University of Illinois at Chicago, Chicago, IL 60607, USA

K. Rukseree
National Center for Genetic Engineering and Biotechnology (BIOTEC), National Science and Technology Development Agency, Thailand Science Park, Pathumthani 12120, Thailand

P. R. Wheeler
Veterinary Laboratory Agency, Weybridge, New Haw, Addlestone, KT15 3NB Surrey, UK

Abbreviations

TB	Tuberculosis
FBPase	Fructose 1,6–bisphosphatase
Ni– NTA	Nickel-nitrilotriacetic acid
SDS-PAGE	Sodium dodecyl sulphate-polyacrylamide gel electrophoresis
PCR	Polymerase chain reaction
kDa	Kilodalton
IPTG	Isopropyl-b-D-thiogalactopyranoside
FPLC	Fast performance liquid chromatography
SEC	Size exclusion chromatography
$NADP^+$	Nicotinamide adenine dinucleotide phosphate
NADPH	Nicotinamide adenine dinucleotide phosphate reduced form
DTT	Dithiothreitol
PGI	Phosphoglucoisomerase
G6PDH	Glucose-6-phosphate dehydrogenase

Introduction

Tuberculosis (TB) is a global public health problem, with 2 billion people, equal to about one-third of the world's population, infected with *Mycobacterium tuberculosis (Mtb)*, the microbe that causes TB. In 2006 over nine million new cases and 1.7 million deaths occurred due to TB [1]. The vast majority of TB deaths are in the developing world, and more than half of all deaths occur in Asia [1]. Current control methods of chemotherapy and vaccination are inadequate, treatment is lengthy, with short-course therapy taking 6 months (DOTS program) and antibiotic resistance presents a serious problem.

One approach to address this problem is to identify new drugs and new drug targets for anti-TB therapy. It is important to understand key metabolism pathways in *Mtb* physiology which enable this adaptable microbe to survive within hostile environment(s) presented by the host (particularly the phagosomal environment) [2]. The enzymes and pathways that are required for growth and survival under the nutritionally restrictive conditions present in the phagosome represent attractive alternative targets for new anti-TB therapies.

Mtb grows on a variety of substrates in vitro but mounting evidence indicates that during infection most of its energy comes from fatty acids [2, 3]. When bacterial metabolism is fueled by fatty acids, synthesis of sugars from intermediates of TCA cycle (particularly the glyoxylate shunt) becomes important for growth and persistence [4–6]. Hence, malate synthase and isocitrate lyase are considered potential targets for the development of new antibacterial agents [7–10]. Phosphoenolpyruvate carboxykinase (PEPCK) the enzyme connecting the TCA cycle and gluconeogenesis, catalyses the reversible decarboxylation and phosphorylation of oxaloacetate (OAA) to form phosphoenolpyruvate (PEP). The PEPCK-encoding gene *pckA* is upregulated by acetate or palmitate but down regulated by glucose. Deletion of the *pckA* gene of *Mycobacterium bovis* BCG led to a reduction in the capacity of the bacteria to infect and survive in macrophages [11]. A recent study demonstrated that PEPCK plays a pivotal role in the pathogenesis of tuberculosis, as it is essential for growth and survival of *Mtb* during infections in mice and that *Mtb* relies primarily on gluconeogenic substrates for in vivo growth and persistence [12]. Except for these recent studies, the role of gluconeogenesis in *Mtb* pathogenesis remains largely unaddressed. Therefore understanding the key structural and functional aspects of enzymes in the gluconeogenic pathway becomes important.

Fructose-1, 6-bisphosphatase (FBPase, EC 3.1.3.11), a key enzyme of gluconeogenesis, catalyzes the hydrolysis of fructose 1, 6-bisphosphate to form fructose 6-phosphate and orthophosphate. This reaction is the opposite of that catalyzed by phosphofructokinase in glycolysis, and the catalytic product, fructose 6-phosphate, is an important precursor in various biosynthetic pathways generating important structural components of cell wall and glycolipids in mycobacteria. In all organisms, gluconeogenesis is an important metabolic pathway that allows the cells to synthesize glucose from noncarbohydrate precursors, such as organic acids, amino acids, and glycerol. FBPases are members of the large superfamily of lithium-sensitive phosphatases, which includes both the inositol phosphatases and FBPases. These enzymes demonstrate bivalent metal-dependent and lithium-sensitive phosphatase activity [13].

Until recently, five different classes of FBPases have been identified based on their amino acid sequences (FBPases I to V) [14–16]. Eukaryotes possess only the FBPase I-type enzyme, but all five types exist in various prokaryotes. Many organisms have more than one FBPase, mostly the combination of types I and II. The type I FBPase is the most widely distributed among living organisms and is the primary FBPase in *Escherichia coli*. An additional class II FBPase is encoded by the *glpX* gene in *E. coli*, which is part of the glycerol 3-phosphate regulon [14]. The completion of the genome sequence of *Mtb* allowed the identification of genes that were predicted to encode enzymes for most central metabolic pathways [17]; however no FBPase was initially assigned. Results from genetic and biochemical analyses revealed that the *Rv1099c* gene of *Mtb* encodes the missing mycobacterial FBPase (II) [13]. The protein encoded by the *Mtb glpX (Rv1099c)* gene is identical to other class II FBPase from *E. coli* (GlpX) (42% identity) [18] and *Corynebacterium glutamicum* FBPase II (65% identity) [19]. Moreover the *glpX (Rv1099c)* transposon mutant was predicted to be attenuated in Transposon Site Hybridization (TraSH) experiments [20], indicating a probable role of this enzyme in mycobacterial pathogenesis.

Since the *Mtb* FBPase II constitutes the only known FBPase in *Mtb* and has no human homologue, biochemical and structural studies could reveal certain unique characteristics of *Mtb* FBPase II that can be exploited for species-specific drug design. Attempts to purify this enzyme were made in the past, however the purified protein was found to be enzymatically inactive. The expression, purification and enzymatic characterization of the functionally active recombinant *Mt* FBPase II is presented here.

Materials and Methods

Materials

Unless otherwise stated, all chemicals were of analytical grade and purchased from Fischer Scientific Company, USA. Restriction endonuclease and T4 DNA ligase were obtained from New England Biolabs, USA. Coupling enzymes for activity assay (yeast glucose-6-phosphate dehydrogenase and yeast phosphoglucoisomerase), Lysozyme and DNAse I were purchased form Sigma Aldrich USA. Plasmid pET15b expression vector and Ni–NTA agarose beads were from Novagen, USA. QIA quick spin columns, plasmid purification kit were from Qiagen, Germany. Complete EDTA-free protease-inhibitor was obtained from Roche Molecular Biochemicals, USA. Hiload 16/60 and Hiload 26/60 FPLC columns packed with Superdex-200 were from GE life sciences. Gel filtration standard used for molecular weight estimation was purchased from Bio-Rad USA. SDS-PAGE was

performed using 4–12% NuPAGE Bis-Tris gradient gels from Invitrogen, USA. SeeBlue Plus2 and SimplyBlue SafeStain were purchased from Invitrogen, USA. Pierce 660 nm Protein Assay kit was procured from Pierce Thermo Scientific, USA. *Escherichia coli* (*E. coli*) DH5α and BL21 (DE3) strains were obtained from Novagen, USA.

Cloning of MtFBPase

The cloning of mycobacterial *glpX* gene for recombinant expression of FBPase was essentially the same as described previously [13].

PCR amplification of the *glpX* gene was carried out using gene specific primers that were designed using the genome sequence of *Mtb* H37Rv from www.webtb.org (forward *Rv1099c*-NdeI 5-GGAATTCCATATGGAGCTGGTCCGGGT-3 and reverse *Rv1099c*-XhoI 3-TGACTCGAGGGCAATGGGTACACG-5).

These primers introduced an NdeI site at the 5′ end and an XhoI at the 3′ end (*Nde*I and *Xho*I sites underlined) to allow the gene to be cloned in-frame into the expression vector pET-15b. Genomic DNA isolated from *Mtb* H37Rv was used as template. The primers were each used at 300 nM final concentration. PCR was carried out using the Mastercycler pro PCR machine (Eppendorf) with *Mtb* DNA as the template and DMSO at 2%. The temperature cycle used was: an initial 3 min at 94 °C to denature high-GC DNA; 10 cycles of 45 s at 94 °C, 1 min at 63 °C and 1 min at 72 °C; 25 cycles of 45 s at 94 °C, 1 min at 63 °C and 1 min at 72 °C (this last 1 min step increasing by 20 s per cycle); and finally an extension step of 7 min at 72 °C to complete primer extension. The PCR amplified product, purified using Qiagen mini columns (Qiagen, Germany) as per manufacturer's instructions, was digested with *Nde*1 and *Xho*1, and ligated using T4 DNA ligase to plasmid pET15b previously digested with the same restriction enzymes as per manufacturers instructions. The ligation mixture was used to transform *E. coli* DH5α cells (Novagen, USA) and selected on LB-Agar plates containing ampicillin (100 μg/ml). Recombinant colonies were analyzed by restriction digestion with *Xho*I and *Nde*I for the release of the insert. For recombinant expression of *Mt*FBPase, *Escherichia coli* BL21 (DE3) (Novagen, USA) was transformed with the plasmid pET15b-*glpX* and selected on LB-Agar plates containing ampicillin (100 μg/ml).

Expression and Purification of MtFBPase in E.coli

E. coli BL21 (DE3) harboring pET15b-FBPase was grown at 37 °C in 100 ml of LB broth containing 100 μg/mL ampicillin overnight. The following day, 10 ml of the broth was transferred to 1 L of LB broth containing 100 μg/mL ampicillin and growth at 37 °C was continued until the OD_{600} was about 0.5. Isopropyl-D-1-thiogalactopyranoside (IPTG) to a final concentration of 0.5 mM was used to induce the culture. The culture was further grown for 8 h at 25 °C and then centrifuged at 4000 g for 20 min at 4 °C. The induction and growth conditions (IPTG concentration, induction temperature and time) were optimized in order to obtain high cell density and high protein expression. Cells were washed with phosphate-buffered saline and stored at −20 °C until further use. The cell pellets collected from the 4-L (4 flasks of 1-L volume) culture were gently stirred at 4 °C for 45 min by the addition of buffer A (50 mM sodium phosphate buffer, pH 8.0, and 300 mM NaCl) +0.50 mg/ml of lysozyme, 2 U/ml of DNAse I (Sigma-Aldrich, USA) and Complete EDTA-free protease-inhibitor (Roche Molecular Biochemicals, USA). The lysed cell pellet was subjected to disruption by sonication on ice using a Branson 450 Sonifier for a total time of 20 min using a fixed protocol (1 pulse/s with the duty cycle dial at 50%). Insoluble

cell debris was removed by centrifugation at 16,000 g for 30 min at 4 °C. The supernatant was filter clarified through a 0.45 μm PVDF syringe filter (Millipore, USA) and loaded onto Ni-NTA bind resin (Novagen, USA) preequilibrated in Buffer A (50 mM sodium phosphate buffer, pH 8.0, and 300 mM NaCl) with 10 mM imidazole. *Mt*FBPase bound to the Ni-NTA column, which was then washed with 32 column volumes of buffer A plus 20 mM imidazole followed by 40 column volumes of buffer A plus 50 mM imidazole. *Mt*FBPase was eluted from the column with 6 column volumes of buffer A plus 250 mM imidazole. The eluate was immediately subjected to buffer exchange and concentration in an Amicon-15 Ultracel 100 K (Millipore, USA) centrifuge concentrator against an exchange buffer (20 mM tricine, 50 mM KCl, 1 mM $MgCl_2$, 0.1 mM DTT, 15% (v/v) glycerol, pH 7.7) prior to running size exclusion chromatography (SEC) as described for FBPase II from *Corynebacterium glutamicum* [19]. *Mt*FBPase was applied to a Superdex-200 Hiload 26/60 column (GE Healthcare Biosciences, USA) on an ÄKTA purifier FPLC system (GE Healthcare Biosciences, USA) pre-equilibrated with the same exchange buffer and eluted at a low flow rate of 1 mL/min. Fractions of 3 ml volumes were collected and pooled according to the chromatogram and the observed purity profile on SDS-PAGE. The pooled fractions were concentrated and filtered through a 0.22-μm membrane filter. For analytical purpose, equal volumes of different purification stage samples were analyzed by SDS–PAGE using 4–12% NuPAGE Bis-Tris gradient gels (Invitrogen, USA), staining was performed using SimplyBlue SafeStain (Invitrogen, USA). All protein purification steps were performed at 4 °C. The protein concentration was estimated by the Thermo Scientific Pierce 660 nm protein assay kit using bovine serum albumin (BSA) as the standard following the instructions of manufacturer.

Native Molecular Weight Estimation by Size Exclusion Chromatography

SEC was performed on an ÄKTA purifier FPLC system using a Hiload 16/60 packed with Superdex 200 (GE Lifesciences). Mobile phase used was 20 mM Tricine, pH 7.7, 50 mM KCl, 1 mM $MgCl_2$ and 0.1 mM DTT. Gel filtration standard from Bio-Rad was used for calibration of the column. Gel filtration standard included thyroglobulin (bovine) 670 kDa, gamma globulin (bovine) 158 kDa, ovalbumin (chicken) 44 kDa, myoglobulin (horse) 17 kDa and vitamin B12 1350 Da. Times of protein elution/retention were determined by monitoring the absorbance at 280 nm. *Mt*FBPase was injected at a concentration of 1.0 mg/ml. Flow rate was set at1 ml/min. The relative elution was calculated as: $K_{av} = (V_e - V_0)/(V_t - V_0)$, where V_e is the elution volume, V_0 is the void volume, and V_t is the total column volume. A standard curve was plotted as K_{av} vs. log (molecular weight). The molecular weight for *Mt*FBPase was estimated from this standard curve obtained using the gel filtration standards.

Determination of Enzyme Activity

Fructose 1,6–bisphosphatase activity was determined using a coupled spectrophotometric assay as described previously[19] by monitoring the increase in absorbance due to the reduction of $NADP^+$ to NADPH at 340 nm. Standard assays were performed in a 96 well plate format in 100 μl reaction mixture aliquots containing 50 mM KCl, 20 mM tricine pH 7.70, 8 mM $MgCl_2$, 1.0 mM $NADP^+$, yeast glucose-6-phosphate dehydrogenase G6PDH (1.0 U/ml), yeast phosphoglucoisomerase PGI(2.5 U/ml) and purified *Mt*FBPase at a concentration of 1 μg/ml (10 μl of 1:100 dilution of 1 mg/ml concentration of the protein added to a final volume of 100 μl reaction mixture). The reaction mixture was

incubated at 30 °C for 10 min and the reaction was started by adding 250 μM of the substrate fructose 1, 6-bisphosphate, followed by monitoring the increase in absorbance at 340 nm at a constant temperature of 30 °C. Fructose 6-phosphate formed by the reaction of FBPase gets converted to glucose 6-phosphate and subsequently to 6-phosphogluconate by coupling enzymes phosphoglucoisomerase and glucose-6-dehydrogenase and the concomitant formation of NADPH (ε340 nm=6.22 mM−1 cm−1) from NADP+ is followed at 340 nm. The activity was measured by monitoring the increase in the absorbance at 340 nm using Spectramax^{384} high throughput microplate spectrophotometer (Molecular devices USA). The reaction was followed for 10 min at a constant temperature of 30 °C.

One unit of FBPase activity is defined as the amount of enzyme that catalyzes the conversion of 1 μmole of fructose 1, 6-bisphosphate to fructose 6-phosphate per minute under the above assay conditions.

Effect of Metal Ions on Enzymatic Activity

The effect of various metal ions on *Mt*FBPase activity was determined by addition of varying amounts of metal ions as their chloride or sulfate salts to the assay mixture followed by measuring the enzymatic activity. Most of the Li^+ sensitive phosphatases (FBPase and IMPase) are strongly inhibited by submillimolar concentrations of Li^+[19, 21–24], we tested the effect of lithium chloride salt by incorporation into the assay mixture in a concentration range 0–40 mM. Effect of bivalent metal ions Mg^{2+} and Mn^{2+} was determined by incorporation of various amounts (concentration range 0.01 mM–40 mM) of these ions (as chloride salts) in the activity assay. Other bivalent metal ions Ca^{2+}, Zn^{2+}, Fe^{2+}, Cu^{2+}, Co^{2+}, Ni^{2+} as their chloride or sulfate salts were also tested in a concentration range 0–40 mM in order to measure their ability to effectively substitute for magnesium in the assay mixture. While these bivalent metal ions were tested, the existing Mg^{2+} in the protein solution was buffer exchanged (using a Amicon-15 Ultracel 100 K (Millipore, USA) with each of the bivalent metal ions respectively. Doing this buffer exhange ensured that there was no background enzymatic activity arising from presence of Mg^{2+} and the observed activity if any was solely due to the presence of the respective bivalent metal ion. Effect of monovalent metal cations K^+ and Na^+ on enzymatic activity was measured by incubating these metals as their chloride salts in the assay mix. Effect of NH_4Cl and KH_2PO_4 (Phosphate is also the catalytic product of FBPase reaction) was also determined by addition of different amounts of these salts in the enzyme assay.

Determination of pH Optima for MtFBPase

For measurement of pH optima, enzyme activity was assayed in 100 mM buffer(s) of various pH values in the range of 5–11 (pH 5.0–6.0, acetate buffer; pH 7.0–9.0, Tris/Tricine buffer pH 10.0–11.0 bicarbonate buffer).

Determination of Thermal Stability

Thermal stability of *Mt* FBPase was studied by incubating the purified protein at different temperatures for 30 min. Upon completion of incubation time, the samples were transferred immediately to ice until determination of residual enzymatic activity and were compared to the activity of unheated (stored at 4 °C throughout) controls.

Determination of Kinetic Properties of MtFBPase

For determination of kinetic constants (*Vmax* and *Km*), the concentration of the substrate fructose 1, 6-bisphosphate in the assay was varied between 3.9 and 1500 μM (Precisely the following concentrations 1500, 750, 500, 250, 125, 62.5, 31.25, 15.625, 7.8125, 3.90625 μM). The reaction rates were followed by monitoring the increase in absorbance at 340 nm as described under enzymatic activity determination. Kinetic parameters were determined by non-linear curve fitting method using GraphPad Prism software (version 5.00, Graph-Pad Software).

Results and Discussion

Cloning, Expression and Purification of *Mt*FBPase

In order to produce recombinant His-tagged *Mt*FBPase protein in *E. coli*, *glpX* gene encoding mycobacterial FBPase was cloned into pET15b, a T7 promoter based inducible bacterial expression vector. Thus the *Mtb* FBPase was expressed as a fusion protein with an N-terminal histidine tag. The sequencing of plasmid was performed at Regional Resources Centre (genetics facility) to confirm that no mutation was introduced during cloning. Significant expression of *Mt*FBPase was observed upon induction with 0.5 mM IPTG in the *E. coli* cell cultures transformed with pET15b vector construct harboring the *glpX* gene (Fig. 1a. Lane 3). No prominent band was detected in the uninduced control (without IPTG) indicating that efficient expression was induced by IPTG (Fig. 1a. Lane 2). To verify whether the *Mt*FBPase is expressed in soluble form or in inclusion bodies, the induced *E. coli* cells were disrupted by sonication, centrifuged and the resulting pellet and supernatant

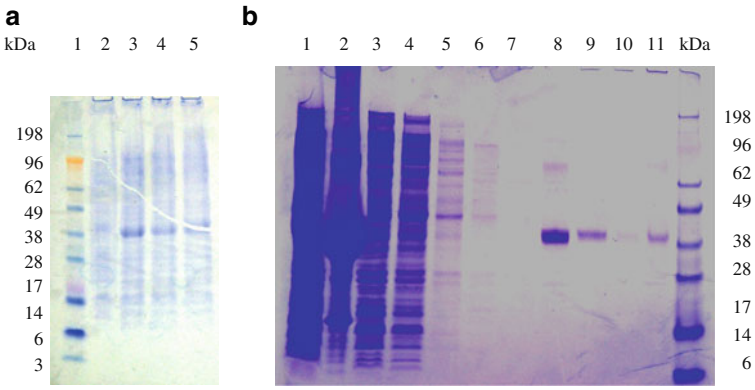

Fig. 1 **a** SDS-PAGE analysis of induction and localization of recombinant *Mt*FBPase. Recombinant *Mt*FBPase was expressed in *E. coli* strain BL21(DE3) and subjected to SDS-PAGE using 4–12% NuPAGE Bis-Tris gradient gels. The gel was stained with SimplyBlue Safe Stain. Lane 1: marker SeeBlue Plus2; Lane 2: uninduced cell lysate; Lane 3: induced cell lysate with 0.5 mM IPTG; Lane 4: soluble fraction; Lane 5: insoluble fraction. **b**: Lane 1: Lysis supernatant; Lane 2: pellet post lysis; Lane 3: Ni-NTA Flow through; Lane 4: Wash 1 concentration 25 mM Immidazole; Lane 5: wash 2 concentration 25 mM immidazole; Lane 6: Wash 3 concentration 50 mM Immidazole; Lane 7: Blank; Lane 8: Ni-NTA elute 250 mM immidazole (immediately dialyzed with Mg++ containing buffer); Lane 9: *Mt*FBPase SEC main peak fractions pooled; Lane 10: Filtrate left after buffer exchange; Lane 11: *Mt*FBPase with other high molecular weight impurities (rejected fractions in SEC); Lane 12: Marker

were analyzed. The mycobacterial FBPase (II) overexpressed in *E. coli* was present in the soluble fraction (Fig. 1a. Lane 4) as well as the insoluble fraction (inclusion bodies). The Ni-NTA elute was relatively impure (Fig. 1b. Lane 8) with some high molecular weight impurities and hence a step of SEC was introduced to purify the protein to homogeneity (Fig. 1b. Lane 9).

Absolute Requirement of Bivalent Metal Ions

The Ni-NTA elute was subjected to enzymatic assay (as described in methods) to measure the FBPase activity, however no activity was obtained initially. Infact this loss of activity has been reported earlier [13]. In case of *C. glutamicum* FBPase purification, the fact that only 16% of the FBPase activity present in the crude extract could be purified was attributed to the absence of Mn^{2+} during elution [19]. In case of *Mt*FBPase we observed that the enzymatic activity was retained if the protein was immediately exchanged with an exchange buffer containing bivalent metal ion magnesium. The fact that no FBPase activity was present in the initial Ni-NTA elute, could be attributed to the absence of Mg^{2+} during elution. Thus for stabilization, the protein solution (post Ni-NTA elution) was immediately exchanged in an exchange buffer containing Mg^{2+}. In order to further purify the protein, the buffer exchanged protein solution was applied onto a Superdex-200 Hiload 26/60 FPLC column.

The recombinant *Mt*FBPase was purified to homogeneity using a two step procedure comprising of Ni-NTA affinity capture followed by SEC. Approximately 1.90 mg of active enzyme with a specific activity of 1.308 U/mg was purified per liter of *E. coli* culture (Table 1). Introduction of the His tag at N-terminal proved effective for affinity capture of the recombinant protein. Moreover the presence of N-terminal his tag did not interfere with catalytic activity as demonstrated for several other FBPases. GlpX protein from *E. coli* was also purified as N-terminal his tagged protein and the crystal structure revealed that the N-terminal residues do not constitute the catalytic pocket of the enzyme [18].

Native Molecular Weight as Determined by Size Exclusion Chromatography

The apparent protein subunit size as determined by SDS-PAGE analysis was about 39 kDa (Fig. 1b) which is higher than the predicted theoretical mass of about 34.5KDa. However

Table 1 Purification of *Mt*FBPase from *E. coli* BL21 (DE3) [pET15b-*glpX*] cells in a 1 l culture

Purification step	Protein (mg)	Total activity Units (U)	Sp. Act. (Units/mg) or μmol/min/mg[a]	Purification fold[b]	Yield (%)[c]
Cell lysate supernatent	347.1	6.42 U	0.019	1.0	100.0
Ni-NTA Elute (Buffer exchanged)	3.3	3.13 U	0.955	51.6	48.8
Final purified protein	1.9	2.49 U	1.300	70.7	39.0

[a] Specific activity defined as Units/mg. A unit of activity catalyzes the formation of 1 μmol of Fructose-6-P per min

[b] Purification fold obtained by comparing specific activities at each stage of purification to that of cell lysate supernatant sample

[c] % yield calculated by comparing the total units (U) at each stage of purification to that of cell lysate supernatant sample

mass spectral analysis of the protein sample revealed the mass of *Mt*FBPase to be 36612.5 Da (accounting for the extra hexa-histidine tag). This abnormal electrophoretic mobility has been cited for some other FBPases [19] as well IMPases such as *Mtb* SuhB [25], and *E. coli* SuhB [26]. Based on several citations, this observed abnormal electrophoretic mobility appears to be a striking feature of the super-family of lithium-sensitive phosphatases because it is also shared by the rice 3′(2′),5′-diphosphonucleoside 3′(2′)-phosphohydrolase (DNPPase, RHL protein) [27].

Molecular weight estimation by SEC calibrated against the elution volumes of known protein standards is an established procedure. SEC is also capable of providing an estimation of the oligomeric state of the protein in solution under the selected buffer conditions. Void Volume of the column as determined by dextran blue V_0=39.80 ml; Total column volume V_t (also referred to as geometric column volume) =120 ml. Using this method we estimated the molecular weight for the purified *Mt*FBPase to be about 127 KDa (Fig. 2), indicating that at a concentration of 1 mg/ml, it exists as an oligomer (i.e. more than one monomer subunit of about 36 kDa). Infact in case of GlpX from *E. coli* an anomalously high native molecular mass of 118 kDa was obtained in the gel filtration experiments (predicted monomer mass=36KDa) indicating that it could be an elongated dimer, this data was further supported by the observed elongated shape of the GlpX dimer in the crystal structure [18]. On a contrary, the purified His-tagged *C. glutamicum* FBPase (65% identity to *Mt* FBPase) eluted at about 140 kDa in size exclusion chromatography indicating it to be a tetramer [19]. The exact oligomeric state of the protein might be difficult to predict from the presented SEC data, however the data indicates that it exists as an oligomer (i.e. more than one monomer subunit of about 36 kDa). Structural information as obtained for GlpX from *E. coli* would provide a better understanding on the anomalously high native molecular mass and also the exact oligomeric state of *Mt*FBPase.

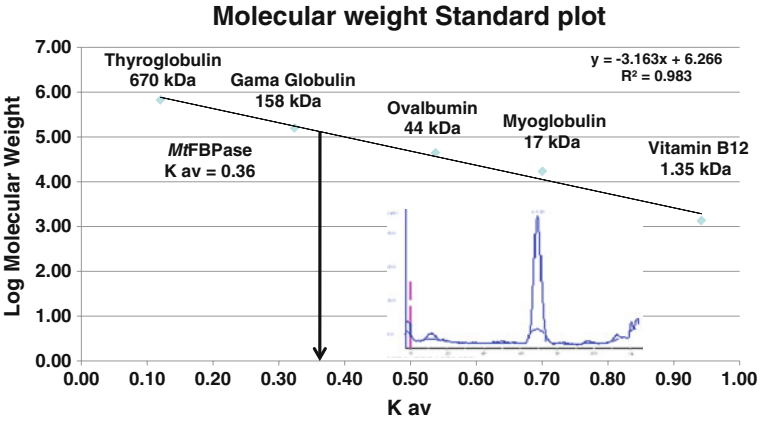

Fig. 2 K_{av} vs log (molecular weight) plot for molecular weight standard. The elution volumes of standard proteins were used to calculate the K_{av} values ($K_{av} = (V_e - V_0)/(V_t - V_0)$). The standard proteins of known molecular weight were thyroglobulin (bovine) 670 kDa, gama globulin (bovine) 158 kDa, ovalbumin (chicken) 44 kDa, myoglobulin (horse) 17 kDa and vitamin B12 1350 Da. Inset: Size-exclusion chromatography (SEC) of *Mt*FBPase on Superdex-200. K_{av} for *Mt*FBPase=0.36

Activity and Stability

The enzymatic activity of the purified enzyme was determined by continuously monitoring the increase in absorbance due to the reduction of $NADP^+$ to NADPH at 340 nm for 10 min. Different amounts of the purified *Mt*FBPase were checked for activity. The activity of the *Mt*FBPase was linearly dependent on the amount of protein added to the reaction mix indicating that initial velocity is proportional to the total enzyme concentration. The minimum concentration of protein giving linear increase in absorbance at 340 nm for 10 min (0.1 μg/100 μl) was used for subsequent assays. The assay was standardized so that all reactants were in excess and only the recombinant *Mt*FBPase was the limiting factor in the reaction. The purified enzyme could be easily stored under refrigeration (2–8 °C) for a period of 1 month without any significant drop in enzymatic activity.

Effect of Bivalent Metal Ions

Like other lithium sensitive phosphatases (FBPase and IMPase) *Mt*FBPase too had an absolute requirement of bivalent metal ions Mg^{2+} and Mn^{2+}. The concentration required for maximal FBPase activity was at least 8 mM and the activity remained steady until a concentration of 40 mM (5-fold) (Fig. 3b). This result was not consistent with those observed for *glpX* from *E. coli* [14, 18] which require much lower concentrations Mg^{2+} for activity. Further mammalian IMPases (human, rat and bovine) [24, 27] and *E. coli* IMPase [26] are inhibited at much lower concentrations of Mg^{2+} (3–5 mM). Infact this magnesium dependence of activity for this particular FBPase resembles the IMPase enzymes from *Mtb* SuhB [25], hypertheromphilic bacteria such as *Thermotoga maritime* [28], archea such as *M. jannaschii* MJ0109 [29] and dual specificity FBPase and IMPase (*Rv2131*) from *Mtb* [30]. Replacement of Mg^{2+} with 4 mM Mn^{2+} led to a 4-fold increase in activity, but presence of Mn^{2+} at higher concentrations led to a decrease in this effect (Fig. 3b). Omission of Mg^{2+} (in assay mixture) resulted in >90% loss of activity. Addition of EDTA at an equimolar concentration to the bivalent metal ions, gave similar results. This establishes the absolute requirement of the bivalent metal ions Mg^{2+} and Mn^{2+}. . Among the other divalent metal ions tested, the only ion that could substitute for Mg^{2+} was Mn^{2+}. However, other divalent metal ions, including Co^{2+}, Ni^{2+}, Cu^{2+}, Zn^{2+}, Fe^{2+} and Ca^{2+}, showed no significant activation of FBPase at any specific concentration (in the range of 0.01 mM–40 mM) in the absence of Mg^{2+}, Fig. 3a shows the relative *Mt* FBPase activities in the presence of each of these bivalent metal ions at concentrations of 8 mM respectively.

Effect of Monovalent Cations (Li+ inhibition)

The monovalent cation Li^+ is a potent inhibitor of the FBPase and IMPase family enzymes [19, 21–24]. In this study, *Mt*FBPase activity was inhibited by Li^+ exhibiting 50% residual activity (IC_{50}) at 200 μM and <10% activity at (IC_{90}) 2.5 mM Li^+. The inhibition constant for LiCl (IC_{50}=200 μM) is in close agreement with that observed for *C. glutamicum* FBPase II [19] (IC_{50}=140 μM) and also with that for mammalian FBPase (0.3 mM). These findings suggest that *Mt*FBPase belongs to the group of lithium sensitive phosphatases, unlike the *glpX* encoded FBPase in *E. coli* which belongs to the more lithium resistant sub group [18]. The observed inhibition constant is significantly lower than that reported previously [13] for *Mt*FBPase cell free extracts (IC_{50}=1.1 mM, IC_{90}=10 mM), possibly due to interference by other components in the cell free extract. In order to determine inhibition specificity of Li^+, other monovalent cations including Na^+ and K^+ were also tested. The

results showed that K^+ had no significant effect on FBPase activity even at 100 mM. Na^+ showed 27% inhibition in enzyme activity at a concentration of 80 mM. Among the other ions tested, NH_4^+ (added as NH_4Cl) did not inhibit activity in a concentration range of 0.1 mM–20 mM. Inorganic phosphate present at a concentration of 2 mM in the enzyme assay displayed 63% maximal activity as compared to control, indicating product (phosphate) dependent inhibition of enzyme activity.

Effect of pH (activity dependence) and Temperature (stability)

The FBPase activity vs pH plot exhibited bell shaped curve (Fig. 4a). The relative activities at respective pH values in comparison to the one at pH 7.7 is plotted. FBPase was active over a pH range from 7 to 9, exhibiting maximum activity at a pH 9.0. However all assays were performed at pH 7.7(physiologically relevant pH) since the enzyme was purified and stored at pH of 7.7 and also found to be stable at pH 7.7. The thermal stability was tested from 10 to 80 °C by incubating the enzyme for 30 min. The enzyme retained its full activity

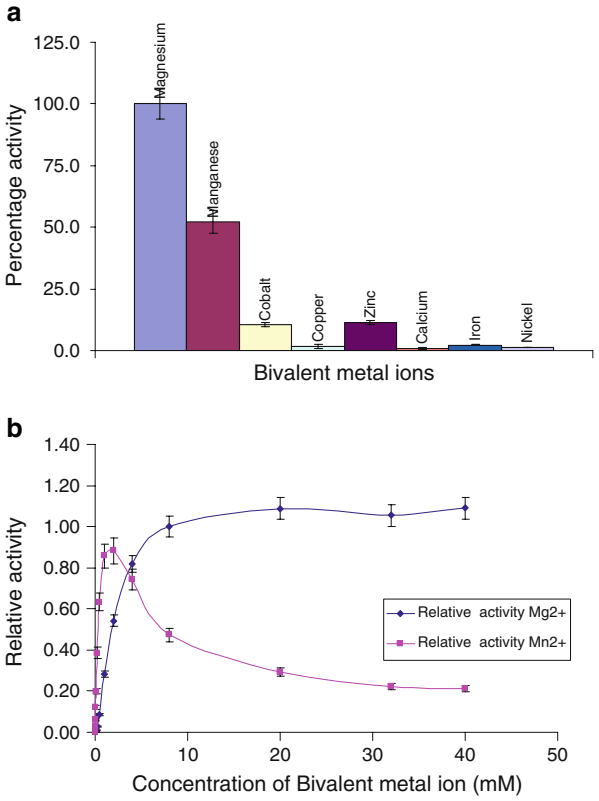

Fig. 3 **a** Metal ion dependence of *Mt* FBPase activity. The activities represented were determined as described in material and methods at 8 mM concentration of each cation and are normalized (percentage activity) to the corresponding value obtained with 8 mM $MgCl_2$, Metal ions Mg^{2+}, Mn^{2+}, Zn^{2+}, Ca^{2+}were used as chloride salts and Co^{2+}, Cu^{2+}, Fe^{2+}, Ni^{2+} were used as sulfate salts; **b** Mg^{2+} and Mn^{2+} dependence of *Mt*FBPase activity; FBPase activity (relative activity to that at 8 mM Mg^{2+}) was assayed as described in material and methods, the concentrations of bivalent metal ions were varied in the range of 0.01–40 mM

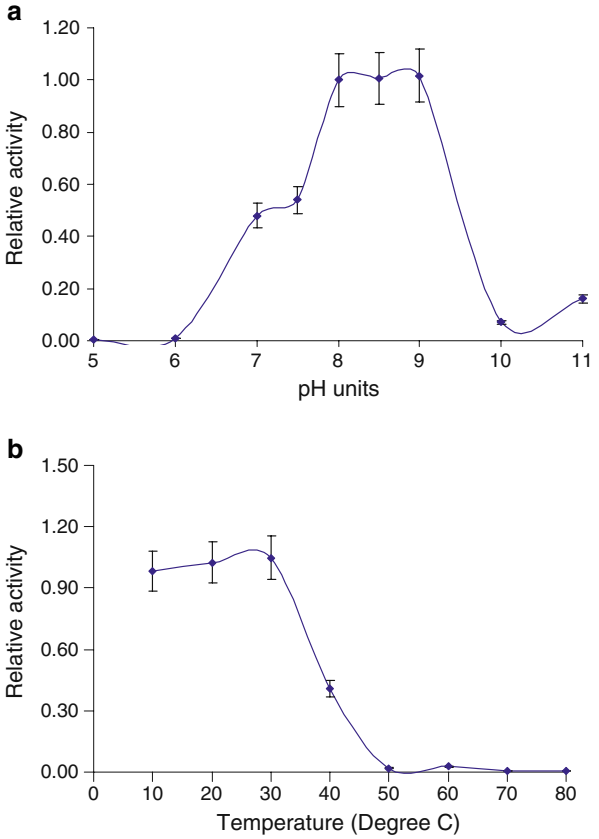

Fig. 4 **a** pH optima for *Mt*FBPase. For measurement of pH optima, enzyme activity was assayed in 100 mM of different buffers (Ref. Methods), Relative activity compared to that of Tricine buffer pH 7.7 is indicated in the plot; **b** Thermostability of *Mt*FBPase was assayed after incubating aliquots of the enzyme in temperature range of 10–80 °C for 30 min followed by determination of residual activity. Relative activity compared to that of the control incubated at 4 °C is shown in the plot

until 30 °C. A significant loss in the activity (65% loss) was noted at 40 °C. Complete inactivation of the enzyme occurred at temperatures greater than 50 °C (Fig. 4b).

Catalytic Properties

For determination of the *Km* and *V*max, the assays contained fructose 1, 6-bisphosphate at concentrations of 3.9–1500 μM. Substrate dependent inhibition of enzymatic activity was observed at concentrations higher than 500 μM. Such substrate dependent inhibition has also been observed for *E. coli* GlpX protein, such a phenomenon was further verified using the malachite green assay for quantification of the phosphate released as was done for *E. coli* GlpX protein. Cooperative behavior with regard to substrate concentration and Mg^{2+} concentration was indeed observed (Fig. 3b. in fact shows that the activity does not change significantly after 8 mM concentration of Mg^{2+}). The double-reciprocal plots of the reaction velocity versus Mg^{2+} (data not shown) were found to be nonlinear at lower concentrations of Mg^{2+}. The plots were

nonlinear because of the co-operative behavior of Mg^{2+} binding to the enzymes. Such a co-operative behavior has been observed for FBPase from other sources as well.

Kinetic parameters were determined by nonlinear curve fitting from the Lineweaver-Burk plot using GraphPad Prism software (version 5.00, Graph-Pad Software).

A k_m of 44 μM, V_{max} of 1.6 U/mg and k_{cat} of 1.0 s^{-1} were determined. The observed k_m of 44 μM indicates high substrate affinity as evident in several other Class II FBPases (*E. coli* GlpX k_m=35 μM [14], *C. glutamicum* FBPase II k_m=14 μM [19]) and *E. coli* Class I FBPase k_m=14 μM [31]. The specific activity and turnover number is lower than that for other reported Class II FBPases. Accordingly the calculated catalytic efficiency k_{cat}/k_m was 1.0/44 μM=22.7 s^{-1} mM^{-1} which is significantly lower than that for the *C. glutamicum* FBPase (k_{cat}/k_m=236 s^{-1} mM^{-1} determined at 30 °C). However it is almost similar to that for GlpX *E. coli* (k_{cat}/k_m=57 s^{-1} mM^{-1} determined at room temperature) and about 40 fold lower than that for *E. coli* FBPase I (k_{cat}/k_m =948 s^{-1} mM^{-1}).

We have successfully cloned, expressed and purified *glpX* encoded FBPase and characterized its activity. The robust expression, purification and activity testing protocols presented here ensure enough production of *Mt*FBPase (in milligram quantities) as deemed necessary for carrying out crystallization trials for structural biology and screening inhibitors in the high-throughput format. The availability of a purified Class II FBPase offers the advantage to test known effectors of Class I FBPase (AMP and Glucose 6-phosphate are inhibitors, citrate and PEP are activators) using incubation assays and complement this data with structural information of the enzyme to help better understand the sites of allosteric regulation (if any) and the mechanism of regulation of class II FBPase (if any) in an organism like *Mtb* where the class I FBPase is absent [31–34]. In order to further understand the relationship between the structure and function of *Mt*FBPase, such as the role of known FBPase effectors, Li^+ inhibition; it becomes imperative to obtain the structure of the enzyme. Crystallogenesis of the protein has been achieved and we are working towards improving the crystal quality and diffraction. It is now our aim to elucidate the crystal structure of *Mt*FBPase and understand its regulation mechanism. Availability of structure of this important enzyme would also offer the leverage to design inhibitors using the rational drug discovery approach.

Acknowledgements We would like to acknowledge Maxwell Rutter for technical assistance with experimental work and proof reading of the manuscript; Prof. Michael Johnson, Dr. Cele Abad-Zapatero and Dr. Shahila Mehboob for providing facility, equipment and technical assistance to perform size exclusion chromatography for protein purification; Prof. Chuan He and Pedro Brugarolas for providing facility, equipment and technical assistance to perform molecular weight estimation of the purified protein. The authors are thankful to American Lung Association (Grant No. RG-82534-N).

References

1. WHO, World Health Organization (2008) Global tuberculosis control: surveillance, planning, financing. WHO Report.
2. Russell, D. G., Cardona, P. J., Kim, M. J., Allain, S., & Altare, F. (2009). *Nature Immunology, 10*, 943–948.
3. Boshoff, H. I., & Barry, C. E., 3rd. (2005). *Nature Reviews. Microbiology, 3*, 70–80.
4. McKinney, J. D., Honer zu Bentrup, K., Munoz-Elias, E. J., Miczak, A., Chen, B., Chan, W. T., et al. (2000). *Nature, 406*, 735–738.
5. Munoz-Elias, E. J., & McKinney, J. D. (2005). *Natural Medicines, 11*, 638–644.
6. Dunn, M. F., Ramirez-Trujillo, J. A., & Hernandez-Lucas, I. (2009). *Microbiology, 155*, 3166–3175.
7. Sharma, V., Sharma, S., Hoener zu Bentrup, K., McKinney, J. D., Russell, D. G., Jacobs, W. R., Jr., et al. (2000). *Nature Structural Biology, 7*, 663–668.

8. Smith, C. V., Huang, C. C., Miczak, A., Russell, D. G., Sacchettini, J. C., & Honer zu Bentrup, K. (2003). *The Journal of Biological Chemistry, 278*, 1735–1743.
9. Anstrom, D. M., & Remington, S. J. (2006). *Protein Science, 15*, 2002–2007.
10. Purohit, H. J., Cheema, S., Lal, S., Raut, C. P., & Kalia, V. C. (2007). *Infectious Disorders Drug Targets, 7*, 245–250.
11. Liu, K., Yu, J., & Russell, D. G. (2003). *Microbiology, 149*, 1829–1835.
12. Marrero, J., Rhee, K. Y., Schnappinger, D., Pethe, K., & Ehrt, S. (2010). *Proceedings of the National Academy of Sciences of the United States of America, 107*, 9819–9824.
13. Movahedzadeh, F., Rison, S. C., Wheeler, P. R., Kendall, S. L., Larson, T. J., & Stoker, N. G. (2004). *Microbiology, 150*, 3499–3505.
14. Donahue, J. L., Bownas, J. L., Niehaus, W. G., & Larson, T. J. (2000). *Journal of Bacteriology, 182*, 5624–5627.
15. Nishimasu, H., Fushinobu, S., Shoun, H., & Wakagi, T. (2004). *Structure, 12*, 949–959.
16. Hines, J. K., Fromm, H. J., & Honzatko, R. B. (2006). *The Journal of Biological Chemistry, 281*, 18386–18393.
17. Cole, S. T., Brosch, R., Parkhill, J., Garnier, T., Churcher, C., Harris, D., et al. (1998). *Nature, 393*, 537–544.
18. Brown, G., Singer, A., Lunin, V. V., Proudfoot, M., Skarina, T., Flick, R., et al. (2009). *The Journal of Biological Chemistry, 284*, 3784–3792.
19. Rittmann, D., Schaffer, S., Wendisch, V. F., & Sahm, H. (2003). *Archives of Microbiology, 180*, 285–292.
20. Sassetti, C. M., & Rubin, E. J. (2003). *Proceedings of the National Academy of Sciences of the United States of America, 100*, 12989–12994.
21. York, J. D., Ponder, J. W., & Majerus, P. W. (1995). *Proceedings of the National Academy of Sciences of the United States of America, 92*, 5149–5153.
22. Patel, S., Martinez-Ripoll, M., Blundell, T. L., & Albert, A. (2002). *Journal of Molecular Biology, 320*, 1087–1094.
23. Albert, A., Yenush, L., Gil-Mascarell, M. R., Rodriguez, P. L., Patel, S., Martinez-Ripoll, M., et al. (2000). *Journal of Molecular Biology, 295*, 927–938.
24. McAllister, G., Whiting, P., Hammond, E. A., Knowles, M. R., Atack, J. R., Bailey, F. J., et al. (1992). *The Biochemical Journal, 284*(Pt 3), 749–754.
25. Nigou, J., Dover, L. G., & Besra, G. S. (2002). *Biochemistry, 41*, 4392–4398.
26. Chen, L., & Roberts, M. F. (2000). *Biochemistry, 39*, 4145–4153.
27. Peng, Z., & Verma, D. P. (1995). *The Journal of Biological Chemistry, 270*, 29105–29110.
28. Chen, L., & Roberts, M. F. (1999). *Applied and Environmental Microbiology, 65*, 4559–4567.
29. Chen, L., & Roberts, M. F. (1998). *Applied and Environmental Microbiology, 64*, 2609–2615.
30. Gu, X., Chen, M., Shen, H., Jiang, X., Huang, Y., & Wang, H. (2006). *Biochemical and Biophysical Research Communications, 339*, 897–904.
31. Kelley-Loughnane, N., Biolsi, S. A., Gibson, K. M., Lu, G., Hehir, M. J., Phelan, P., et al. (2002). *Biochimica et Biophysica Acta, 1594*, 6–16.
32. Hines, J. K., Chen, X., Nix, J. C., Fromm, H. J., & Honzatko, R. B. (2007). *The Journal of Biological Chemistry, 282*, 36121–36131.
33. Hines, J. K., Fromm, H. J., & Honzatko, R. B. (2007). *The Journal of Biological Chemistry, 282*, 11696–11704.
34. Hines, J. K., Kruesel, C. E., Fromm, H. J., & Honzatko, R. B. (2007). *The Journal of Biological Chemistry, 282*, 24697–24706.